

# Isotropic microwave composites with negative refraction

C.R. Simovski<sup>1</sup> and B. Sauviac<sup>2</sup>

August 28, 2018

<sup>1</sup>St. Petersburg Institute of Fine Mechanics and Optics, Russia

<sup>2</sup>DIOM Laboratory (*D*e*vices and I*n*strumentation for O*ptoelectronics and *M*icrowaves),  
Université Jean Monnet, Saint Etienne, CEDEX 42023, France

## Abstract

The properties of artificial isotropic microwave composites which would possess simultaneously negative permittivity and permeability are studied theoretically. Four kinds of composites are considered. Two of them concern media with split-ring resonator particles with different particle arrangements. The other two are realized with Omega particles. An analytical antenna model of the electromagnetic behavior of a split-ring resonator (SRR) is suggested and verified by numerical simulations. Next, material parameters of composite media made with SRR or Omega particles are calculated. It is shown that the Omega-composites are more prospective for obtaining negative real values of permittivity and permeability than the split-ring resonators.

## 1 Introduction

V. G. Veselago studied in sixties [1] the electromagnetic properties of materials whose permittivity and permeability have negative real parts simultaneously. He showed that these media exhibit unusual effects like anomalous negative refraction of electromagnetic waves and existence of backward waves (when the group velocity and the Poynting vector are directed opposite with respect to the phase velocity). This concept implies many other interesting features of wave propagation that were reviewed in [1].

These *Veselago* media do not exist in nature. The interest in creating such media artificially, for optical applications, has been indicated by J. Pendry in [2]. This kind of medium can be obtained with arrays of conducting inclusions of a special shape. It is obvious that the response of these materials will be resonant. Therefore, negative refraction is possible only within a more or less narrow frequency band (or bands) [3]. This "negative" band can be a part of a resonant band of inclusions that are used in the composite. This is quite clear analyzing the Lorentz model of the resonant dispersion.

At this stage of studies, since it is easier to use resonant inclusions with millimeter dimensions, it seems to be reasonable to focus on applications for the microwave region of

the spectrum (optic composites will need micrometer particles) and to study their response experimentally. How to prepare these composites in a best way? Which shape of inclusions is more suitable? These are the general questions addressed by this article.

Works that have theoretically predicted negative permittivity for composite media have been reviewed in [4]. However, publications containing the same results for the permeability are not so common. In [5] and [6] it was indicated that it was a very difficult problem to obtain a magnetic resonant response of inclusions (in order to get a negative real part of  $\mu_{eff}$ ). Probably, it was the reason for which these authors have chosen a rather complicated particle named as *split-ring resonator (SRR)*, see Fig. 1. They maintained in these works, that SRR has only a resonant magnetic polarizability and no resonant electric one.

In [6] it was suggested that to obtain negative permittivity simultaneously with negative permeability. SRR inclusions must be combined with a lattice of straight wires. This complex system is a very cumbersome technical solution. The only special case where wave propagates normally to the wires (which corresponds to [7]) is suitable to observe the negative refraction in such a structure. It is clear that the structures from [6] cannot be considered as an *isotropic* backward-wave composite.

In this paper we show that the SRR particles alone allow to obtain simultaneously negative permeability and permittivity. Indeed, these inclusions also possess a resonant electric polarizability that has not been discovered in [5] and [6]. We also point out that the analytical model of SRR suggested in [5] does not give a satisfactory explanation of the frequency behavior of effective permeability. Moreover, it is possible to realize an *isotropic* composite with negative refraction choosing properly the geometry, arrangement and concentration of SRR particles in a host dielectric matrix.

However, we have found that SRR is not the best choice for obtaining a backward-wave medium at microwaves. Actually, the resonant electric response of SRR is weaker than the magnetic one. We show that it is better to use an inclusion known as Omega particle (or  $\Omega$ -shaped conducting particle) suggested in 1992 by Saadoun and Engheta [8] since its magnetic and electric responses are of the same order.

Numerical and analytical modeling of Omega particles have been recently made in [9]-[12] and the properties of uniaxial and planar Omega composite media have been derived. It appears that these media are prospective for creating low-reflecting shields and antenna radomes in microwave applications. With this kind of objectives, in 1995-1996, we studied theoretically uniaxial Omega composites and noticed that sometimes the real parts of both permittivity and permeability became negative, especially in the cases with high densities of particles. Thus, as it was not suitable for our goals, the experimental samples of Omega composites which were prepared under guidance of S.A. Tretyakov [9] were dilute mixtures in order to avoid the apparition of negative properties. Negative permittivity and permeability of Omega composites has been predicted in the paper [13]. However, the model of the material parameters presented in this work and based on the transmission-line model of Omega particle was contradictory (particle size was taken of the order  $\lambda$  but the constitutive relations were introduced as if the composites were continuous media) and violated some physical foundations (Kramers-Kronig relations, etc).

In the following we consider the effective properties of isotropic composites of both Omega and SRR particles embedded in a dielectric host medium. We study two different kinds of particles arrangement. The first one is a mixture with a random orientations of particles.

The second one is obtained by positioning the particles at the sides of a cubic unit cell, like it is shown in Figs 2 and 3. Different inclusions and structures are finally compared.

## 2 Theory

Both SRR particles and Omega particles are bianisotropic particles. In other words, an external electric field produces a magnetic dipole in the particle and, at the same time, an external magnetic field produces an electric dipole. For SRR, this magnetoelectric effect is reduced by choosing the opposite positioning of the splits of both loops. However, it cannot cancel out exactly since the loops are of different sizes.

Let a SRR particle be located in an infinite and homogeneous dielectric medium with permittivity  $\epsilon$ . Consider the electromagnetic response of an individual SRR particle to local magnetic and electric fields. The polarizabilities of a SRR particle are dyadic coefficients relating the local electric and magnetic fields  $\mathbf{E}^{\text{loc}}$ ,  $\mathbf{H}^{\text{loc}}$  with the induced electric and magnetic dipole moments:

$$\mathbf{p} = \bar{a}_{ee} \cdot \mathbf{E}^{\text{loc}} + \bar{a}_{em} \cdot \mathbf{H}^{\text{loc}} \quad (1)$$

$$\mathbf{m} = \bar{a}_{me} \cdot \mathbf{E}^{\text{loc}} + \bar{a}_{mm} \cdot \mathbf{H}^{\text{loc}} \quad (2)$$

The electric and magnetic moments of the SRR as a whole are vector sum of the moments induced in the outer and inner loops (indices 1 and 2, respectively) :

$$\mathbf{p} = \mathbf{p}_1 + \mathbf{p}_2 \quad (3)$$

$$\mathbf{m} = \mathbf{m}_1 + \mathbf{m}_2 \quad (4)$$

In this section we evaluate analytically the polarizabilities of a SRR particle, assuming that the inclusion is fabricated from a round wire of radius  $r_0$ . The section of the wire is small enough to satisfy the inequality  $r_0 \ll a_{1,2}$ , where  $a_{1,2}$  are the averaged radiuses of rings 1 and 2 (see Fig. 1a). Distance  $\delta$  between the broken ends of each ring is assumed to be small compared to  $a_{1,2}$ . The analytical model of the Omega particle will not be reproduced here. Analytical antenna theory and its verification can be found in [10].

Finally, using the calculated polarizabilities we derive for each kind of particles the material parameters through the well-known Maxwell Garnett model.

### 2.1 SRR particle eigenfrequencies

We consider the SRR particle as a pair of two mutually coupled resonant scatterers. The complex amplitudes of induced currents at the splits of both rings can be written as follows:

$$I_1(Z_{C1} + Z_{L1}) + I_2 Z_{12} = \mathcal{E}_{H1} + \mathcal{E}_{E1}, \quad (5)$$

$$I_2(Z_{C2} + Z_{L2}) + I_1 Z_{12} = \mathcal{E}_{H2} + \mathcal{E}_{E2} \quad (6)$$

Indices 1 and 2 refer to the outer and inner ring respectively.  $\mathcal{E}_H$  and  $\mathcal{E}_E$  are the electromotive forces induced by the external fields.  $I_{1,2}$  are the currents at the splits of the rings.  $Z_{L1,L2}$  represent the inductive loop impedances ( $Z_{L1,L2} = j\omega L_{1,2}$ ), and  $Z_{C1,C2}$  are the capacitive

impedance ( $Z_{C_1, C_2} = 1/(j\omega C_{1,2})$ ) of the slits. For a magnetic field excitation we can neglect the individual loop capacitance which has only a small influence. For the study of electric polarization, influence of the proper capacitance of one loop must be taken into account. For that we use the known theory of a split loop antenna [16] and [15] which takes into account the capacitive properties of an individual loop scatterer and its radiation losses.  $Z_{12}$  in (5),(6) is the mutual impedance of broken loops. We have chosen to include directly the capacitive mutual coupling in the term  $C_{1,2}$ . Otherwise the analytical model of mutual coupling would become too involved. With these considerations the mutual impedance  $Z_{12}$  in (5),(6) is expressed only as a mutual inductance  $M$  ( $Z_{12} = j\omega M$ ).

The capacitances  $C_{1,2}$  are composed of two contributions. The first part  $C_S$  originates from the splits of each loop. The second one is due to capacitive coupling of loops and can be seen as a consequence of the following effect. Consider first as a reference the conductor of one loop (the outer loop of a SRR particle, for example). Next, place another conductor parallel to the first one (in our case, the inner loop, with the split at the opposite side). Then, assume that one half of the first loop (e.g. the upper part) contains positive charge  $+Q$ , and the second half of the first loop (e.g. the lower part) contains negative charge  $-Q$ . These charges are distributed somehow along the loop perimeter. As the two loops are positioned closely, in the upper half of the second loop, a negative charge  $-q$  is induced. Hence, the distribution of the global charge  $-q$  around the second loop repeats the distribution of  $+Q$  in the first loop. Note that we do not have necessarily the correspondence  $Q = q$ . Of course, the same thing happens in the lower part of the structure, where the induced charge  $+q$  appears. So two equivalent capacitances  $C_{mut}$  arise from this situation as shown in Fig. 4. Hence, we obtain an effective additional capacitance which is equal to  $C_{mut}/2$ , connected in parallel to the proper capacitance of the split. One can note that this equivalent scheme can be improved taking into account that there is an additional capacitance of the second slit. However, we are trying to derive a model of SRR as simple as possible and the complexity, increased by this additional capacitance, is not justified.

Values of inductances  $L_{1,2}$ , mutual inductance  $M$  and total capacitances  $C_{1,2}$  are analytically calculated in Appendix.

To obtain the eigenfrequencies of the SRR particle, we let the right-hand side of (5),(6) vanish and equate the determinant to zero:

$$(Z_{C_1} + Z_{L_1})(Z_{C_2} + Z_{L_2}) - Z_{12}^2 = 0 \quad (7)$$

Equation (7) can be written as

$$\left( \frac{1}{j\omega C_1} + j\omega L_1 + r_1 \right) \left( \frac{1}{j\omega C_2} + j\omega L_2 + r_2 \right) + \omega^2 M^2 = 0 \quad (8)$$

where  $r_{1,2}$  are small resistances that represent the radiation and the Joule losses of both loops. They lead to a small imaginary correction term denoted as  $\kappa(\omega)$  in equation (9):

$$(\omega^2 - \omega_-^2)(\omega^2 - \omega_+^2) + j\kappa(\omega) = 0 \quad (9)$$

If we assume that the SRR particle is perfectly conducting, the term  $\kappa$  describes only the radiation losses of a magnetic dipole and it can be derived from the energy balance condition,

as it was done in [17] for arbitrary dipole scatterers. Comparing (8) with (9) we find the eigenfrequencies:

$$2 \left( \frac{\omega_{\pm}}{\omega_m} \right)^2 = \frac{\omega_m^2}{\omega_1^2} + \frac{\omega_m^2}{\omega_2^2} \pm \sqrt{\left( \frac{\omega_m^2}{\omega_1^2} + \frac{\omega_m^2}{\omega_2^2} \right)^2 - 4} \quad (10)$$

where we denote

$$\omega_m^2 = \frac{1}{\sqrt{C_1 C_2 (L_1 L_2 - M^2)}}, \quad \omega_{1,2}^2 = \frac{1}{C_{1,2} L_{1,2}}$$

Frequencies (10) correspond to two eigenmodes. If the frequencies  $\omega_-$  and  $\omega_+$  differ dramatically the two eigenmodes of the induced current are excited at different frequencies. This leads to two separate resonances (that magnetic and that electric ones) of the particle. However, we will see below that in practical cases  $\omega_+ \approx \omega_-$ . The two resonance bands overlap, and we obtain a result close to that of the Lorentz model with only one resonance, as it goes for simple scatterers. As a consequence, it matches qualitatively the results of [5].

## 2.2 Magnetic polarizability of SRR particle

Next, we are going to derive the polarizabilities of SRR particle using (5),(6) and definitions (1) and (2). First, we study the magnetic polarizability. For a magnetic excitation ( $\mathbf{E}^{\text{loc}} = 0, \mathbf{H}^{\text{loc}} = \mathbf{z}_0 H^{\text{loc}}$ , where the  $z$ -axis is perpendicular to the loop plane as it is shown in Fig. 2) we obtain:

$$\mathcal{E}_{H1,2} = -j\omega\mu_0 S_{1,2} H^{\text{loc}}, \quad m_{1,2} = I_{1,2} \mu_0 S_{1,2} \quad (11)$$

Here  $S_{1,2} = \pi a_{1,2}^2$  are the effective loop areas.

The only component of the magnetic moment is vertical, i.e.

$$\bar{\bar{a}}_{mm} = \mathbf{z}_0 \mathbf{z}_0 a_{mm}^{zz}$$

Then, relations (11) together with (1)-(6) and (7)-(9) lead to the following expression:

$$a_{mm}^{zz} = -D\omega^2 \frac{B_1(\omega^2 - \omega_1'^2) + B_2(\omega^2 - \omega_2'^2)}{\Delta + j\kappa} \quad (12)$$

where we have denoted

$$\begin{aligned} \Delta &= (\omega^2 - \omega_-^2)(\omega^2 - \omega_+^2) \\ B_1 &= S_1(S_1 L_2 - M S_2), \quad B_2 = S_2(S_2 L_1 - M S_1) \\ D &= \frac{\mu_0^2}{L_1 L_2 - M^2} \end{aligned} \quad (13)$$

and

$$\omega_{1,2}'^2 = \frac{\omega_{1,2}^2}{\left(1 - \frac{M S_{2,1}}{L_{2,1} S_{1,2}}\right)} \quad (14)$$

Now let us find the term  $\kappa$ . The theory from [17] based on the balance of received and re-radiated power for any particle with magnetic dipole polarizability  $a_{mm}^{zz}$  gives the equation

$$\text{Im} \frac{1}{a_{mm}^{zz}} = \frac{k^3}{6\pi\mu_0} \quad (15)$$

Comparing this formula with (12) we come to the following expression for the term  $\kappa$ :

$$\kappa = \frac{\omega^2 D k^3 [B_1(\omega^2 - \omega_1'^2) + B_2(\omega^2 - \omega_2'^2)]}{6\pi\mu_0} \quad (16)$$

With an appropriate calculation of inductances and capacitances (see Appendix), it is now possible to completely evaluate the magnetic polarizability  $a_{mm}^{zz}$ .

### 2.3 Electric polarizability of SRR particle

Now we are interested in the electric polarizability. Consider the action of local electric fields on a SRR. Two possibilities exist to induce polarization on the SRR particle.

First, we study the case where the electric field is along the horizontal direction ( $x$ -direction for an individual particle). The only electro-dipole mode of the current is excited in both loops in this case. The induced charges are concentrated at the splits and at the opposite points and the polarizability component  $a_{ee}^{xx}$  is quasi-static. It does not depend on the presence or absence of the split and equations (5),(6) are useless in this case<sup>1</sup>.

In [14] we derived formula (28) for  $xx$ -component of the polarizability of a circular loop with area  $S = \pi a^2$ . Denoting this polarizability as  $a_{QS}$  we obtain from [14]:

$$a_{QS} = -\frac{4S J_1'(ka)}{\omega\eta A_1(ka)}$$

In this equation,  $\eta = \sqrt{\mu_0/\epsilon\epsilon_0}$  is the wave impedance of the host medium,  $k = \omega\sqrt{\mu_0\epsilon\epsilon_0}$  is the wave number in the medium,  $J_1'(ka)$  is the derivative of the Bessel function of the first order,  $A_1(ka)$  is one of so-called King's coefficient known from the theory of loop antennas [15],[16]. King's coefficients with a very high accuracy are approximated in [15] and take the following form:

$$\begin{aligned} A_1(ka) &= \left(\frac{ka - \frac{1}{ka}}{\pi}\right) \left(\log \frac{8a}{r_0} - 2\right) - \frac{0.667(ka)^3 - 0.207(ka)^5}{\pi} \\ &\quad - j0.333(ka)^2 - j(0.133ka)^4 + j0.026(ka)^6 \\ A_0(ka) &= \frac{ka}{\pi} \left(\log \frac{8a}{r_0} - 2\right) + \frac{0.667(ka)^3 - 0.267(ka)^5}{\pi} - j0.167(ka)^4 - j0.033(ka)^6 \\ A_2(ka) &= \left(\frac{ka - \frac{4}{ka}}{\pi}\right) \left(\log \frac{8a}{r_0} - 0.667\right) + \frac{-0.4ka + 0.21(ka)^3 - 0.086(ka)^5}{\pi} \\ &\quad - j0.05(ka)^4 - j0.012(ka)^6 \end{aligned}$$

Since we have two loops, we must sum up their  $a_{QS}$  to obtain the result:

$$a_{ee}^{xx} = -\frac{4S_1 J_1'(ka_1)}{\omega\eta A_1(ka_1)} - \frac{4S_2 J_1'(ka_2)}{\omega\eta A_1(ka_2)} \quad (17)$$

---

<sup>1</sup>Because  $I_{1,2} = 0$  and the electromotive force  $\mathcal{E}_E$  induced at the split is also equal to zero: charges are the same at the edges of each split.

Now we consider the case where the electric field is directed along  $y$ -axis. Here the resonant electric polarization appears in both loops of the SRR particle. To obtain the resulting polarizability, we combine the theory of a single loop with resonant electric polarization (see [16] and [14]) with equations (5) and (6).

In [14] the following formula has been derived for the  $yy$ -component of the electric polarizability of a single loaded loop of radius  $a$ :

$$a_{ee}^{yy} = \frac{4\pi a^2 J_1'(ka)}{\omega\eta A_1(ka)} \left( 1 + \frac{2j}{\pi\eta A_1(ka)} \frac{1}{Y_L + Y_{\text{split}}} \right) \quad (18)$$

Here  $Y_{\text{split}}$  is the admittance that is connected to the loop split. For both loops we have  $Y_{\text{split}} \equiv 1/Z_{\text{split}} = j\omega C_{1,2}$  which include the mutual capacitance of the loops.  $Y_L = 1/Z_L$  is the proper loop admittance. In our case of coupled loops, we should replace  $Y_L$  by the value  $Y_{1,2}$  which takes into account their mutual inductance. For loop 1, we can say that it is composed of the proper impedance of the loop  $Z_{L1}$  and of the additional impedance  $Z_{12}I_2/I_1$ , which is the contribution of loop 2 into loop 1. Then, for loop 1, we have to substitute into (18):

$$\frac{1}{Y_1} = Z_1 = Z_{L1} + Z_{12} \frac{I_2}{I_1}$$

Similarly, for the second loop we have:

$$\frac{1}{Y_2} = Z_2 = Z_{L2} + Z_{12} \frac{I_1}{I_2}$$

Denoting the ratio  $I_1/I_2$  as  $\xi$  and taking into account that  $Z_{12} = j\omega M$ , we come to the following formulas for the  $yy$ -polarizabilities of both loops:

$$a_{e1}^{yy} = \frac{4S_1 J_1'(ka_1)}{\omega\eta A_1(ka_1)} \left( 1 + \frac{2j}{\pi\eta A_1(ka_1)} \frac{1}{Y_1 + j\omega C_1} \right) \quad (19)$$

$$a_{e2}^{yy} = \frac{4S_2 J_1'(ka_2)}{\omega\eta A_1(ka_2)} \left( 1 + \frac{2j}{\pi\eta A_1(ka_2)} \frac{1}{Y_2 + j\omega C_2} \right) \quad (20)$$

where

$$Y_1 = \frac{Y_{L1}}{1 + \frac{j\omega M Y_{L1}}{\xi}}$$

$$Y_2 = \frac{Y_{L2}}{1 + j\omega M Y_{L2} \xi}$$

The proper loop admittance is given by [15]:

$$Y_L = \frac{1}{j\pi\eta} \left( \frac{1}{A_0(ka)} + \frac{2}{A_1(ka)} + \frac{2}{A_2(ka)} \right) \quad (21)$$

Expressions of  $Y_{L1,L2}$  follow from (21) with substitutions  $a = a_{1,2}$ .

Equations (5),(6) allow to find  $\xi$ :

$$\xi = \frac{\mathcal{E}_{E1}(Z_{L2} + Z_{C2}) - \mathcal{E}_{E2}Z_{12}}{\mathcal{E}_{E2}(Z_{L1} + Z_{C1}) - \mathcal{E}_{E1}Z_{12}} \quad (22)$$

If a loop with proper impedance  $Z_L$  loaded with the impedance of the split  $Z_{\text{split}}$  is submitted to an external electric field, an electromotive force is induced. Its value is given by formula (26) from [14]:

$$\mathcal{E}_E = \frac{4aJ'_1(ka)\left(\frac{1}{Y_L} + \frac{1}{Y_{\text{split}}}\right)}{j\eta A_1(ka)} \left(1 + \frac{j}{\pi\eta} \frac{1}{Y_L + Y_{\text{split}}}\right) E_y^{\text{loc}} \quad (23)$$

Substituting the values  $a_{1,2}$  and  $r_0$  into (21) and (23) allows to calculate the electromotive forces induced by an external electric field in each loop of the SRR particle. Then, substituting expressions of  $\mathcal{E}_{E1,E2}$  into (22) with the help of relation (21) we can find  $\xi$ . Consequently, we derive an expression of  $Y_{1,2}$  which is then substituted into (19) and (20). Finally, we evaluate  $a_{ee}^{yy}$  as the sum

$$a_{ee}^{yy} = a_{e1}^{yy} + a_{e2}^{yy} \quad (24)$$

At this point, we have at our disposal a complete analytical model of the electric and magnetic polarizabilities of an individual SRR particle (other components of  $\bar{a}_{ee}$  and  $\bar{a}_{mm}$  are zeros).

## 2.4 Effective polarizabilities of a planar bianisotropic particle in isotropic mixtures

An isotropic mixture with a random orientation of particles can be considered as a mixture realised with isotropic particles which have averaged scalar polarizabilities [19]:

$$a_{ee}^{av} = \sum_{\alpha=1}^3 \frac{a_{ee}^{\alpha\alpha}}{3}, \quad a_{mm}^{av} = \sum_{\alpha=1}^3 \frac{a_{mm}^{\alpha\alpha}}{3}, \quad a_{em}^{av} = a_{me}^{av} = 0 \quad (25)$$

Here we have designated Cartesian components with index  $\alpha = x, y, z$ . The particles under consideration do not have cross components:  $a_{ee}^{\alpha\beta} = 0$  for  $\alpha \neq \beta$ . Moreover, we have seen with our analytical model, that the only polarizabilities that are non-zero are:  $a_{ee}^{xx}$ ,  $a_{ee}^{yy}$  and  $a_{mm}^{zz}$ .

If SRR or Omega particles are arranged on the sides of cubic unit cells (see Figs. 2 and 3), the magnetoelectric effect also disappears and dyadics  $\bar{a}_{em}$ ,  $\bar{a}_{me}$  of the individual particles do not contribute into material parameters. Furthermore, mutual coupling of six particles belonging to the same cell is weak enough if the cell size  $d_{\text{cell}}$  is a bit more than the particle size  $d_p$  (the particles do not touch one another). Now, let us evaluate the equivalent effective polarizability of each kind of unit cell ignoring the mutual coupling between the particles of a cubic cell.

### 2.4.1 Effective polarizabilities of a cubic cell of SRR particles

The cubic cell under consideration is presented Fig. 2. An electric field directed along an arbitrary edge of a cubic cell excites the electric dipoles in four SRR particles. For two particles  $\mathbf{E}^{\text{loc}}$  is parallel to the line connecting the rings splits and corresponds to the polarizability  $a_{ee}^{xx}$ . For the other two particles  $\mathbf{E}^{\text{loc}}$  is perpendicular to this line and corresponds to  $a_{ee}^{yy}$ .



Consider now the magnetic field effect on the cell. A magnetic field directed along an arbitrary edge of a cell induces two equivalent magnetic moments in two opposite particles. So, the magnetic polarizability of a unit cell turns out to be the double of  $a'_{mm}$ .

To summarize, the cubic unit cell is equivalent to an isotropic particle with electric and magnetic polarizabilities given by

$$a'_{ee} = 2a_{ee}^{xx} + 2a_{ee}^{yy}, \quad a'_{mm} = 2a_{mm}^{zz} \quad (26)$$

### 2.4.2 Effective polarizabilities of a cubic cell of Omega particles

For a unit cubic cell of Omega particles (see Fig. 3) the situation is quite different. Here the resonant excitation by the electric field directed along the arms of  $\Omega$  (along  $y$ -axis in the model of an individual particle) is mainly due to the presence of the arms [10]. Therefore the total electric polarization of two opposite omega particles keeps resonant behavior. Within the resonant band the quasi-static component of Omega particle polarizability  $a_{ee}^{xx\Omega}$  describing the response of a particle to the electric field applied normally to the arms (see Fig. 1) is small compared to  $a_{ee}^{yy\Omega}$ . Then one obtains for a unit cell from Omega particles approximate relations

$$a'_{ee} \approx 2a_{ee}^{yy\Omega}, \quad a'_{mm} = 2a_{mm}^{zz\Omega} \quad (27)$$

where  $a_{ee}^{yy\Omega}$ ,  $a_{mm}^{zz\Omega}$  can be taken from [10].

### 2.4.3 Material parameters of composites

The material parameters of the isotropic mixture are given by the standard Maxwell Garnett formulas [19]:

$$\epsilon_{eff} = \epsilon + F \left( \frac{Na'_{ee}}{\epsilon_0} - \frac{N^2 a'_{ee} a'_{mm}}{3\epsilon_0 \mu_0} \right) \quad (28)$$

$$\mu_{eff} = 1 + F \left( \frac{Na'_{mm}}{\mu_0} - \frac{N^2 a'_{ee} a'_{mm}}{3\epsilon_0 \mu_0 \epsilon} \right) \quad (29)$$

In these equations

$$F^{-1} = 1 - \frac{Na'_{ee}}{3\epsilon_0 \epsilon} - \frac{Na'_{mm}}{3\mu_0} + \frac{N^2 a'_{ee} a'_{mm}}{9\epsilon_0 \mu_0 \epsilon}$$

These equations are general for the different kinds of composites we are studying. Depending on the composition of mixture, only expressions for polarizabilities change.

- for *random media*, which are realized by mixing particles in an isotropic and random way in a host medium,  $N$  denotes the concentration of particles, and  $a'_{ee} = a_{ee}^{av}$ ,  $a'_{mm} = a_{mm}^{av}$  are given by (25)
- for *cubic-cell media*, which are obtained with previously mentioned cubic unit cells,  $N$  denotes the concentration of cells, and  $a'_{ee}$  and  $a'_{mm}$  are given by (26) or (27).

### 3 Model validation for SRR particle

Our analytical model is below compared with numerical simulations. Numerical model which allows to simulate the averaged polarizabilities of an arbitrary bianisotropic particle with thin wire of round cross section, that allows to calculate also material parameters of a random composite has been derived from [20], [21]. Since its publication this method has been widely used to simulate bianisotropic composites.

We compared the analytical and numerical models of the SRR prepared with wires of radius  $r_0 = 0.2$  mm. Numerical example presented here corresponds to the following parameters. The averaged radiuses of the inner and outer loops are equal to  $a_2 = 2.1$  and  $a_1 = 2.7$  mm. The length of the broken part is taken  $\delta = 0.1$  mm or  $\delta = 0.4$  mm ( $\delta$  is the same in both loops). The host medium permittivity  $\epsilon = 1.5$ .

In Fig. 5 the real part of  $a_{mm}^{av}$  is shown calculated in both analytical and numerical ways for the case  $\delta = 0.1$  mm. The imaginary parts of  $a_{mm}^{av}$  for this case are shown in Fig. 6. The real and imaginary parts of  $a_{ee}^{av}$  calculated in both ways are shown in Figs. 7 and 8, respectively.

Comparing the resonant frequencies of  $a_{ee}^{av}$  and  $a_{mm}^{av}$ , we can note that the difference is quite negligible. This means that the resonant bands overlap ( $\omega_+ \approx \omega_-$ ) as we mentioned previously.

We can observe also, that the analytical model shows a weak additional resonance for the electric polarization around 5.2 GHz. This is a defect of our analytical theory which is related to the adopted approximations. We think that the second resonance follows from our model of loops mutual coupling which is not accurate enough. Adding a very small imaginary value to the right-hand side of formula (31) we completely suppress this second resonance without changing the values of  $a_{mm}$  and  $a_{ee}$  within the first resonant band. Of course, this correction has nothing to do with the theory but it confirms that the model of  $Z_{1,2}$  is not accurate enough and can be improved.

The electric polarizability calculated in both analytical and numerical ways for the case  $\delta = 0.4$  mm (the other parameters are the same as above) is presented in Fig. 9.

The agreement between two models is quite the same for  $\delta = 0.1$  and  $\delta = 0.4$  mm. The same remarks could be made for  $a_{mm}$ .

Polarizabilities of SRR particle are very sensitive to deviations of the particle parameters, and we can consider that the agreement between the two models is satisfactory. It makes our analytical theory suitable to calculate the effective composite parameters and, hence, allows to solve explicitly the inverse problem for such composites.

### 4 SRR and Omega isotropic composites

In this section we analyze the material parameters of effective media obtained with SRR particles or Omega particles. The mixture is fabricated by

- distributing the particles with random orientations in a host medium
- positioning the particles at the sides of a cubic unit cell (filled by the same medium as the matrix) as shown in Fig. 2 and 3.

## 4.1 SRR composites

In Figs. 10 and 11 both  $\epsilon_{eff}$  and  $\mu_{eff}$  of a *random SRR composite* are shown (calculated in both analytical and numerical ways). Particles geometry and background permittivity has been taken the same as above (the split width is  $\delta = 0.4$  mm). The concentration of particles has been taken  $N = 1$  particle/cm<sup>3</sup>. For the particle maximal size 5.8 mm this concentration allows to use the Maxwell Garnett averaging procedure.

We can observe on Fig. 10 that the permittivity is not becoming negative within the resonant band (whereas both models of the permeability allow the negative values for  $\text{Re}(\mu_{eff})$ ). Here, the permittivity of SRR composite remains positive because of the restriction of dilute mixtures (imposed by the validity of the Maxwell Garnett model).

In the case of *SRR cubic media*, since we apply the Maxwell Garnett model to the unit cells considering them as particles, we can take the concentration of SRR particles greater than in the case of a random mixture, and that, without violating the restriction of dilute mixtures.

As a consequence, in Fig. 12 we can see that  $\text{Re}(\mu_{eff})$  and  $\text{Re}(\epsilon_{eff})$  are negative simultaneously. The concentration of cells has been calculated for the case of unit cells arrangement as presented in Fig. 3. The size of the cell is equal to  $6 \times 6 \times 6$  mm<sup>3</sup>, and the averaged distance between the centers of two adjacent cells is close to 11 mm. This allows to consider the composite with such cells as a dilute mixture.

## 4.2 Omega composites

In Fig. 13 and 14 we present the results calculated within the frame of the Maxwell Garnett model for an Omega composite prepared from cubic units as shown in Fig. 3. In that case, the maximal size of the Omega particle is equal to 6.4 mm. The cell size is equal to  $6.5 \times 6.5 \times 6.5$  mm<sup>3</sup>. For an illustration, we have chosen the following dimensions. The radius of the loop is 3 mm and the radius of the wire is  $r_0 = 0.1$  mm. The length of an arm is  $L = 3$  mm. The host medium permittivity is  $\epsilon = 2$ . Note that for cases when  $\delta \ll a$ , parameter  $\delta$  does not influence the polarizabilities at all (see [10]).

In Fig. 13, the real parts of the permittivity and permeability of the Omega composite versus the frequency are shown. In Fig. 14, the imaginary parts of permittivity and permeability are presented. We can see that  $\text{Re}(\epsilon_{eff})$  and  $\text{Re}(\mu_{eff})$  reach  $-1$  practically at the same frequency. This is a very exciting result if we refer to paper [2] where the perfect lens has been predicted for the case  $\text{Re}(\epsilon_{eff}) = \text{Re}(\mu_{eff}) = -1$ .

The case of *random Omega composite* (Fig. 15) with density  $N = 1$  particle/cm<sup>3</sup> only differs by the heights of the resonant peaks of the permittivity.

## 5 Conclusion

Based on the analysis of electromagnetic phenomena that appear in a *split ring resonator*, we have developed an analytical model of SRR particles. We have shown that the SRR particles can exhibit, on their own, simultaneously magnetic and electric polarizability. The proposed model has been successfully compared with a numerical approach. So, these results point out that previous works on SRR do not give a satisfactory explanation of the behavior

of this particle. Next, we have calculated with the Maxwell Garnett approach the effective parameters of composites realized with SRR particles. We have shown that it is possible to obtain an isotropic composite with negative refraction choosing properly the geometry, arrangement and concentration of SRR particles in a host dielectric matrix. The way of making these composites has been presented. With this technique, we have obtained an effective material with simultaneously negative real part of permittivity and permeability.

However, we have shown that SRR is not the only and not the best choice for obtaining a backward-wave medium at microwaves. Actually, we can obtain the same kind of medium, using Omega particle instead of SRR particles. With these inclusions we have derived a material which gives  $\text{Re}(\epsilon_{eff}) = \text{Re}(\mu_{eff}) = -1$  in the resonant band. This is the wished result exposed by the inventor of the SRR particle. Finally, we can conclude that the Omega particle is a more appropriate choice in order to create microwave composites with negative refraction.

We have to point out yet, that our model exhibits a high level of radiation losses within the resonant band. As a consequence, if material samples are so lossy, it would be problematic to measure the negative refraction on it. These high radiation losses are due to the Maxwell Garnett model which implies a random organization of particles and is consistent with the Kramers Kronig relations. However, the proposed *cubic composite* can be classified in a middle position between random media and lattices. The composite is constructed as a lattice, stacking up cubes in a three dimensional chessboard assembly, but it is not a perfect lattice. There is indeed, a certain random organization in the positions of the particles on the sides of the cubic cells (as it can be seen on figures 2 and 3). So, we can reasonably expect that losses given by the Maxwell Garnett model will be overestimated.

## References

- [1] V.G. Veselago, The electrostatics of substances with simultaneously negative values of  $\epsilon$  and  $\mu$ , *Soviet Physics Uspekhi*, vol. 10, no. 4, pp. 509-514, 1968 (originally published in Russian in *Uspekhi Fizicheskikh Nauk*, vol. 92, No. 3, pp. 517-526, July 1967).
- [2] J.B. Pendry, Negative refraction makes a perfect lens, *Physical Review Lett.*, Vol. 85, No. 18, pp. 3966-3969, 2000.
- [3] S.A. Tretyakov, Meta-materials with wideband negative permittivity and permeability, *Microwave and Optics Technol. Lett.*, Vol. 31, pp. 163-165, 2001.
- [4] S.A. Tretyakov, C.R. Simovski, Negative epsilon, negative mu, etc.: what radio engineers know about that, *Proc. of Electromagnetic Crystal Structures*, T.F. Krauss, Ed., University of St. Andrews, Scotland, June 9-14, 2001.
- [5] J.B. Pendry, A.J. Holden, D.J. Robbins and W.J. Stewart, Magnetism from conductors and enhanced nonlinear phenomena, *IEEE Trans. Microwave Theory Tech.*, Vol. 47, pp. 2075-2081, 1999.

- [6] D.R. Smith, W.J. Padilla, D.C. Vier, S.C. Nemat-Nasser and S. Schultz, Composite media with simultaneously negative permeability and permittivity, *Physical Review Lett.*, Vol. 85, No. 18, pp. 4184-4187, 2000.
- [7] R.A. Shelby, D.R. Smith and S. Schultz, Experimental verification of a negative index of refraction, *Science*, Vol. 292, pp. 77-79, 2001.
- [8] M.M.I. Saadoun and N. Engheta, A reciprocal phase shifter using novel pseudochiral or Omega medium, *Microwave and Optical Technology Letters*, Vol. 5, pp. 184-188, 1992.
- [9] T.G. Kharina, S.A. Tretyakov, C.R. Simovski, A.A. Sochava and S. Bolioli, Experimental study of artificial Omega media, *Electromagnetics*, Vol. 18, No. 3, pp. 437-457, 1998.
- [10] C.R. Simovski, S.A. Tretyakov, A.A. Sochava, B. Sauviac, F. Mariotte, T.G. Kharina, Antenna model for conductive omega particles, *J. of Electromagnetic Waves Applic.*, Vol. 11, No. 11, pp. 1509-1530, 1997.
- [11] S.A. Tretyakov, A.A. Sochava, Eigenwaves in uniaxial chiral and omega media, *Microwave and Optical Technology Letters*, Vol. 6, No. 12, pp. 701-705, 1993.
- [12] S.A. Tretyakov, A.A. Sochava, Reflection and transmission of plane electromagnetic waves in uniaxial bianisotropic materials, *Intern. J. Infrared and Millimeter Waves*, Vol. 15, No. 5, pp. 829-855, 1994.
- [13] M.M.I. Saadoun and N. Engheta, Theoretical studies of electromagnetic properties of non-local Omega media, in *Progress in Electromagnetic Researches*, PIER9, pp. 351-397, 1994.
- [14] S.A. Tretyakov, F. Mariotte, C.R. Simovski, T.G. Kharina and J.-Ph. Heliot, Analytical antenna model for chiral scatterers: comparison with numerical and experimental data, *IEEE Trans. Antennas Prop.* Vol. 47, No. 7, pp. 1006-1015, 1996.
- [15] Antenna Handbook: Theory, Applications and Design, Y.T. Lo and S.W. Lee, Eds., NY: Van Nostrand Reinhold, 1988, ch. 7.
- [16] R.W.P. King, The loop antenna for transmission and reception, in *Antenna theory, Part 1*, R.E. Collin and F.J. Zucker, Eds., NY, McGraw Hill, 1969.
- [17] V.V. Yatsenko, S.I. Maslovski and S.A. Tretyakov, Electromagnetic interaction of parallel arrays of dipole scatterers. In *Progress in Electromagnetic Research'25*, pp. 285-307, 2000. (Abstract also in *J. of Electromagnetic Waves Applic.*, Vol. 13, No. 2, pp. 189-203, 1999).
- [18] P.L. Kalantarov and L.A. Tseitlin, *Calculation of inductances*, Leningrad, Energoatomizdat, 1986 (in Russian).
- [19] F. Mariotte, S.A. Tretyakov, B. Sauviac, Modelling effective properties of chiral composites, *IEEE Antennas Prop. Mag.*, Vol. 38, No. 2, pp. 22-32, 1996.

- [20] F. Mariotte, B. Sauviac and J. Ph. Héiot, Modélisation de matériaux chiraux á structures hétérogenes (modele MTWC) : théorie, validations expérimentales et applications, *Journal de Physique III, France*, Vol. 5, pp. 1537-1564, Octobre 1995.
- [21] F. Mariotte, B. Sauviac and S.A. Tretyakov, Artificial bianisotropic composites, Chapter 18 of the book *Frontiers of Mathematical Methods in Electromagnetics*, R. Mittra and D. Werner, Eds., IEEE Press 2000.
- [22] F. Gardiol, *Electromagnétisme*, Dunod Université, Paris, 1987, p. 51.

## 6 Appendix

Inductance of a round loop of radius  $R$  made with a wire of cross section radius  $r_0$  can be found e.g. in [16]:

$$L = \mu_0 R \left( \log \left( \frac{8R}{r_0} \right) - 2 \right) \quad (30)$$

Inductances of both rings of SRR can be obtained with (30) with the substitution  $R = a_{1,2}$ .

Formula (5.23) from [18] for two concentric loops whose radii  $a_1, a_2$  are close to one another, gives the following approximation for the mutual inductance:

$$M = \mu_0 a_1 \left[ (1 - \chi) \log \left( \frac{4}{\xi} \right) - 2 + \xi \right] \quad (31)$$

where  $\chi = (a_1 - a_2)/2a_1$  is a small parameter ( $0 < \chi < 0.25$ ). In (31) we have neglected the terms of order  $\xi^2$ .

Now, consider the capacitances included in the loops splits. We can write in accordance with Fig. 4

$$C_1 = C_{s1} + \frac{C_{mut}}{2}, \quad C_2 = C_{s2} + \frac{C_{mut}}{2} \quad (32)$$

For  $C_s$  we have the simple equation of a conventional (parallel-plate) capacitor

$$C_s = \frac{\pi r_0^2 \epsilon \epsilon_0}{\delta} \quad (33)$$

if the split width  $\delta$  is much smaller than the wire cross section diameter. Otherwise, if  $\delta \gg r_0$  one has  $C_{s1,2} \ll C_{mut}$  and the capacitance of the split can be ignored. We do not study the cases when  $r_0 \approx \delta$ .

Next, we calculate  $C_{mut}$ . The capacitance per unit length of two parallel wires of diameter  $2r_0$  with the distance between the wire axes  $d = a_2 - a_1$  denoted below as  $C_0$  is known [22]:

$$C_0 = \frac{\pi \epsilon \epsilon_0}{\operatorname{arccosh} \left( \frac{d}{2r_0} \right)} \quad (34)$$

Roughly (but successfully) we can consider  $C_{mut}$  as the capacitance between two equivalent parallel straight wires of length  $\pi a \equiv \pi(a_1 + a_2)/2$  with distance  $d$  between their axes. However, we would obtain a bad result if we simply multiply  $C_0$  by  $\pi a$  in order to find  $C_{mut}$ . We should take into account the non-uniformity of the charge distribution along these

equivalent wires and then write  $C_{mut} = C_0 P$  (where the effective length of two parallel charged wires  $P$  is smaller than  $\pi a$  due to this non-uniformity).

We use the King theory of loop antennas [16] in order to find effective length  $P$ . For it we write the Fourier expansion for the current induced in the reference loop by a magnetic field (with respect to the azimuth angle  $\phi$ ):

$$I(\phi) = I^{(0)} + I^{(1)} \cos \phi + I^{(2)} \sin \phi + \dots \quad (35)$$

It corresponds to the following expansion for the induced charges per unit angle:

$$\tau(\phi) = \tau_1 \sin \phi + \tau_2 \cos \phi + \dots \quad (36)$$

In the King theory it was proven that (for the case of small loop antenna ( $ka_{1,2} \ll 1$ ) with a finite impedance of the split) the omitted terms in expansions (35) and (36) are of the next order of smallness compared to the remained terms [16]. The uniform term  $I^{(0)}$  represents the magneto-dipole mode of the induced current and has nothing to do with induced charges. Two other terms in (35) are responsible for the electric polarization of the loop and are related with the charge distribution. We can rewrite (36) as:

$$\tau(\phi) = \tau_{max} \sin(\phi + \phi_0) \quad (37)$$

where  $\tau_{max} \equiv \sqrt{\tau_1^2 + \tau_2^2}$ . So, at it was already mentioned, half of the loop ( $\phi_0 < \phi < \pi + \phi_0$ ) contains positive charge  $Q$ , and the other half ( $-\pi + \phi_0 < \phi < \phi_0$ ) contains negative charge  $-Q$ . The distribution of these charges is sinusoidal. The induced charges in the other loop have the opposite sign but the same sinusoidal distribution (see also Fig. 4).

We obtain that the distribution of the charge along two effective equivalent parallel wires of length  $\pi a$  is sinusoidal with zeros at the ends of these wires. It leads to the result  $P = 2a$  which gives together with (34) the approximate relation for the capacitance  $C_{mut}$ :

$$C_{mut} = \frac{2\pi\epsilon\epsilon_0 a}{\operatorname{arccosh}\left(\frac{d}{2r_0}\right)} \quad (38)$$

If the loop is excited by  $y$ -polarized electric field, the formula of the current distribution (35) keeps valid [16]. Coefficients  $I^{(0,1,2)}$  change in this case, but the charges  $+Q$  and  $-Q$  remain sinusoidally distributed on the two halves of each the loop. Therefore the formula (38) keeps valid, too.

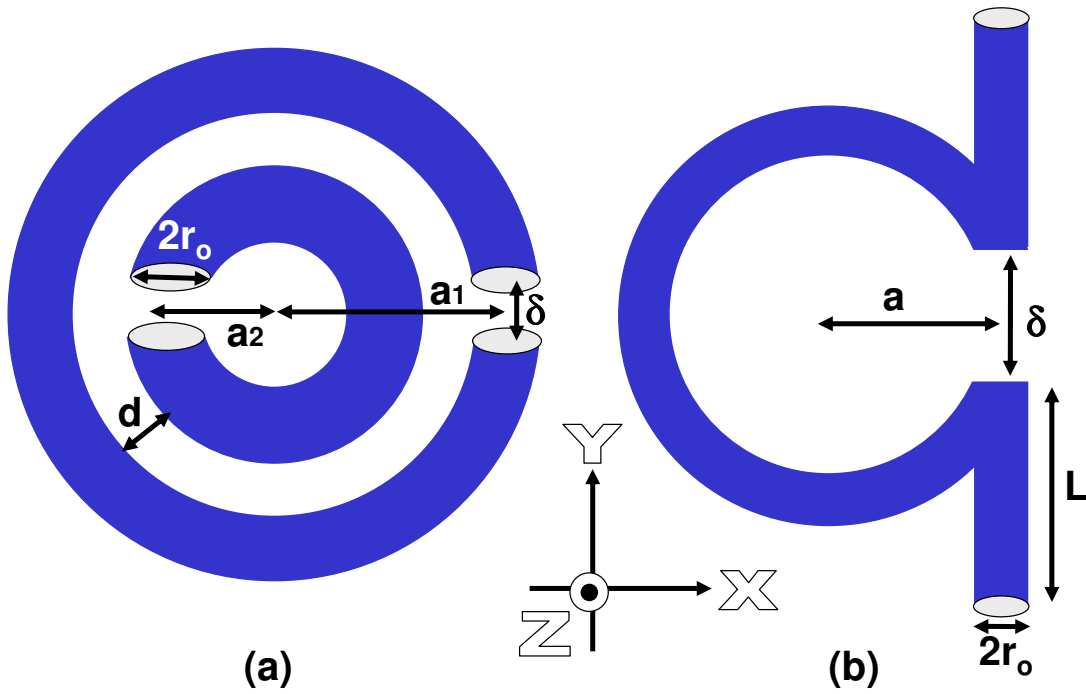


Figure 1: Geometry of particles. (a) SRR particle (b) Omega particle

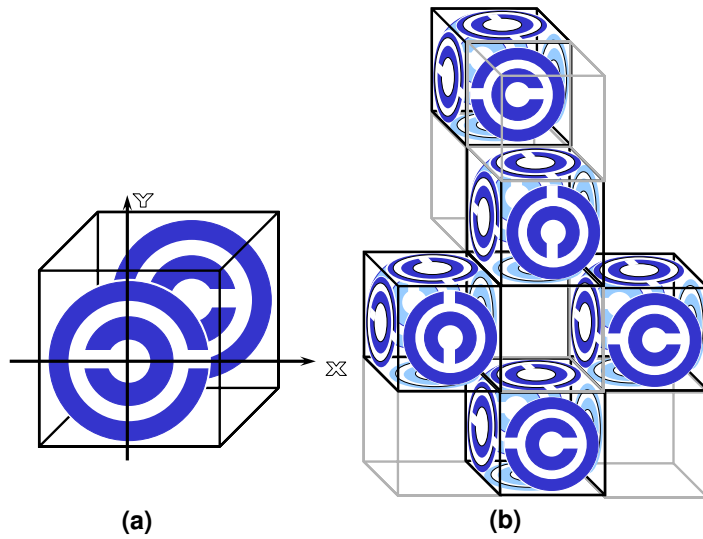


Figure 2: Preparing the isotropic group of SRR particles. (a) A unit cell contains 6 particles. Particles located on opposite side of a cubic cell are rotated by  $180^\circ$ . (b) Composite can be prepared using the principle of chessboard.



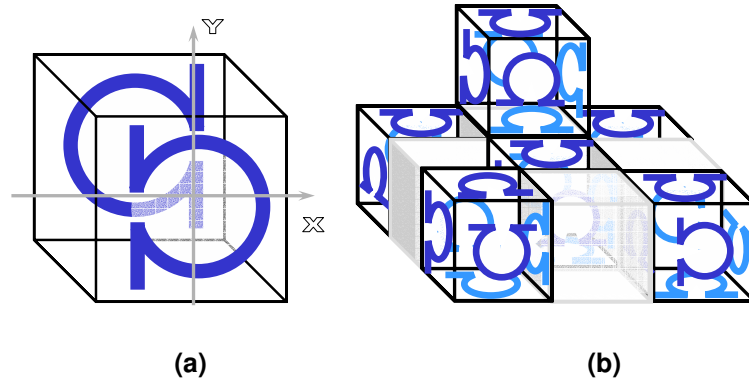


Figure 3: Isotropic group of Omega particles (the same method as in 2). (a) Omega particles are positioned at the sides of a cubic unit cells. (b) The arrangement of unit cells shown here allows to obtain an effectively isotropic medium.

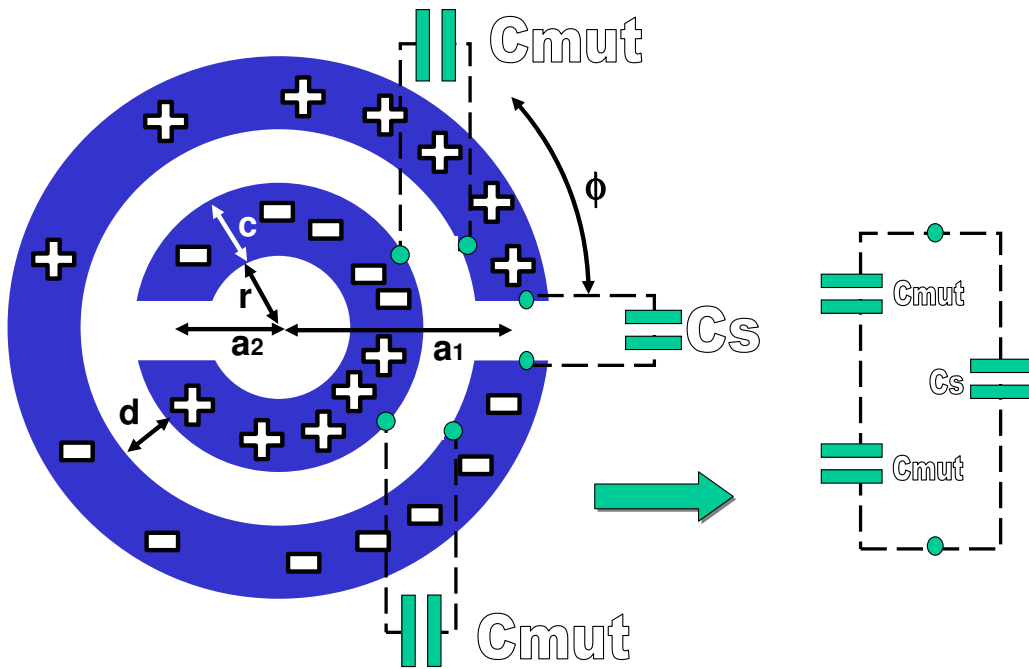


Figure 4: Capacitive mutual influence of loops. The connection of equivalent capacitors  $C_{mut}$  is shown.

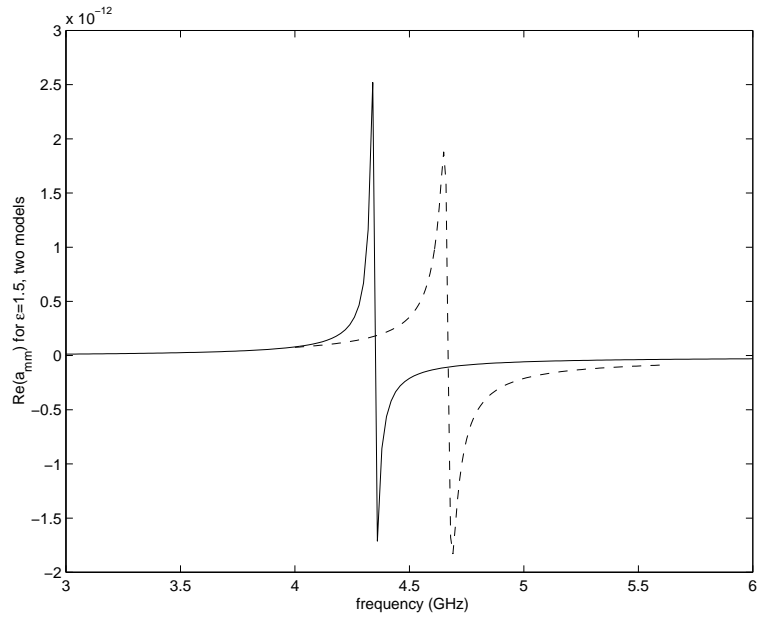


Figure 5: Real part of the averaged magnetic polarizability of SRR versus frequency. The split width  $\delta$  is 0.1 mm. Analytical model (solid) and numerical model (dashed).

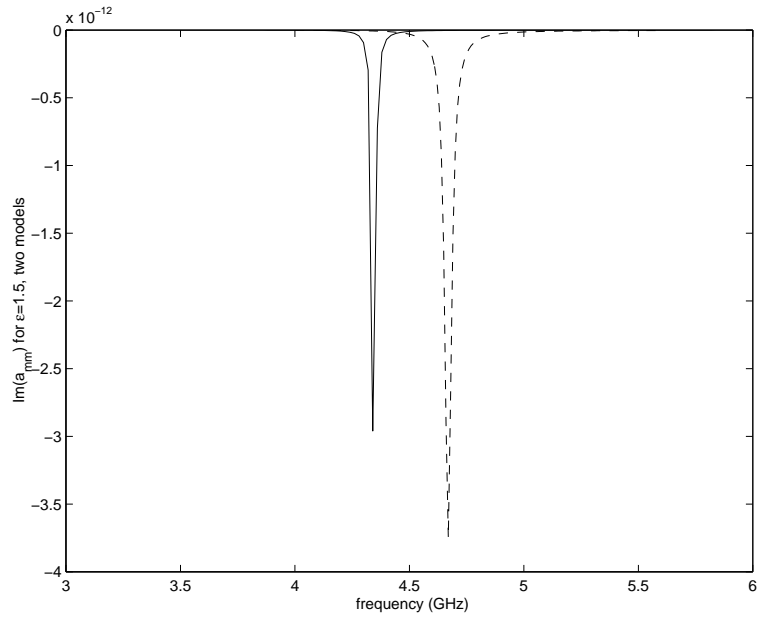


Figure 6: Imaginary part of the averaged magnetic polarizability of SRR versus frequency. The split width  $\delta$  is 0.1 mm. Analytical model (solid) and numerical one (dashed).

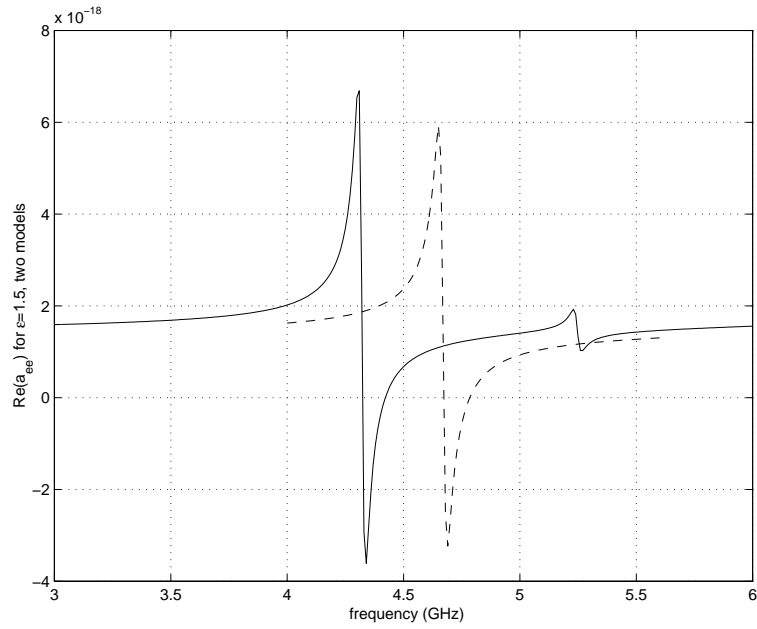


Figure 7: Real part of the averaged electric polarizability of SRR versus frequency. The split width is 0.1 mm. Analytical model (solid) and numerical model (dashed).

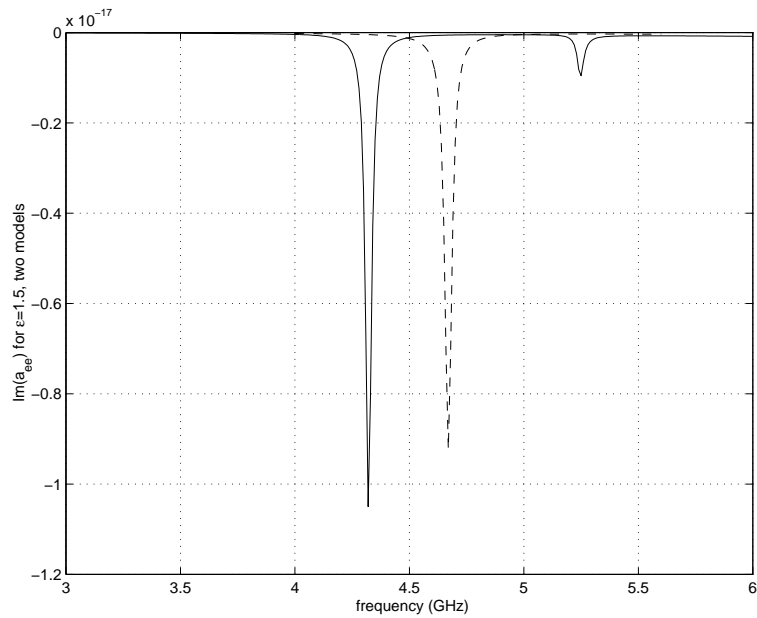


Figure 8: Imaginary part of the averaged electric polarizability of SRR versus frequency. The split width is 0.1 mm. Analytical model (solid) and numerical one (dashed).

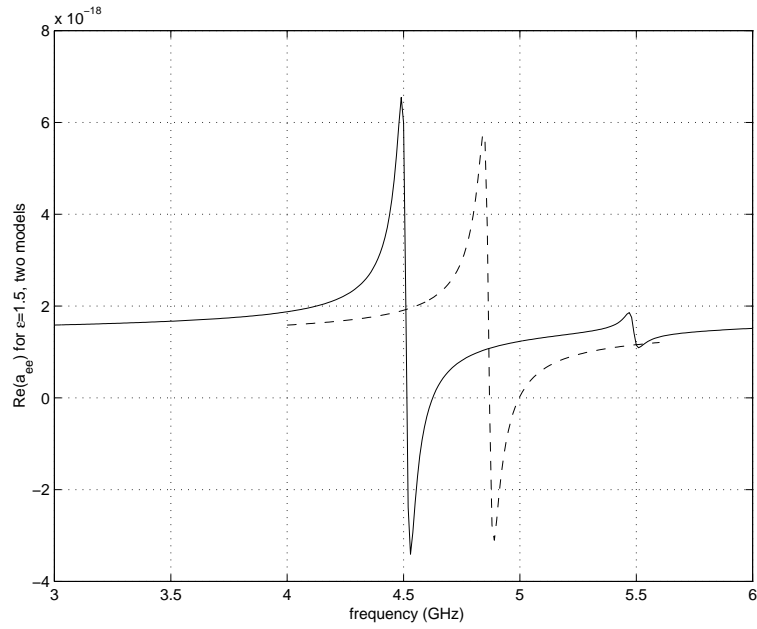


Figure 9: Real part of the averaged electric polarizability of SRR versus frequency. The split width is 0.4 mm. Analytical model (solid) and numerical one (dashed).

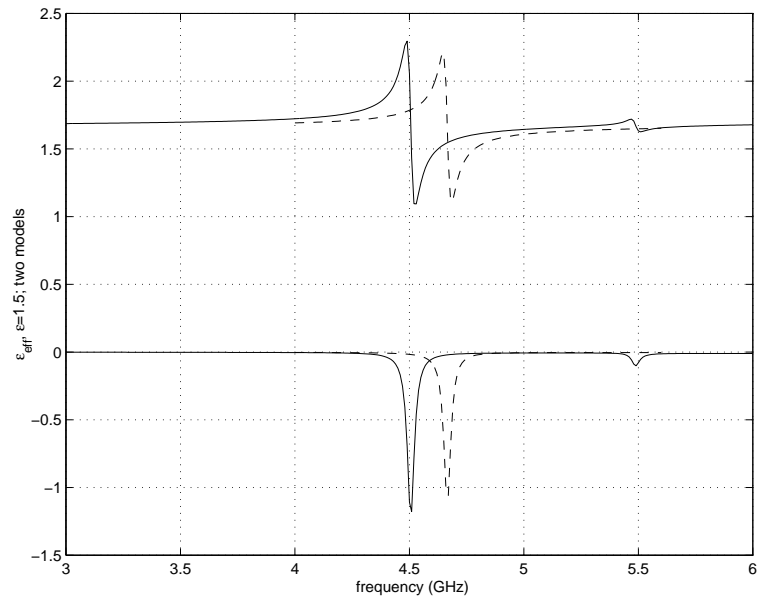


Figure 10: Real and imaginary parts of the permittivity of the random SRR composite versus frequency. Analytical model (solid) and numerical model (dashed).

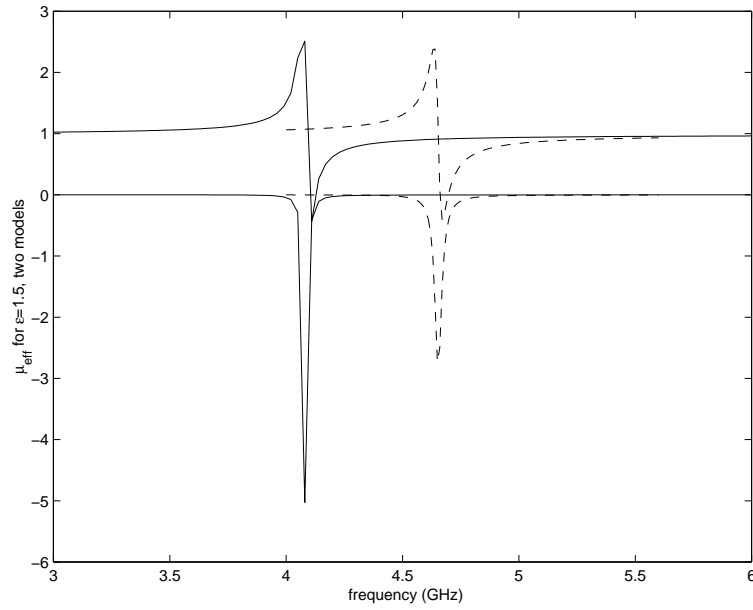


Figure 11: Real and imaginary parts of the permeability of the random SRR composite versus frequency. Analytical model (solid) and numerical one (dashed).

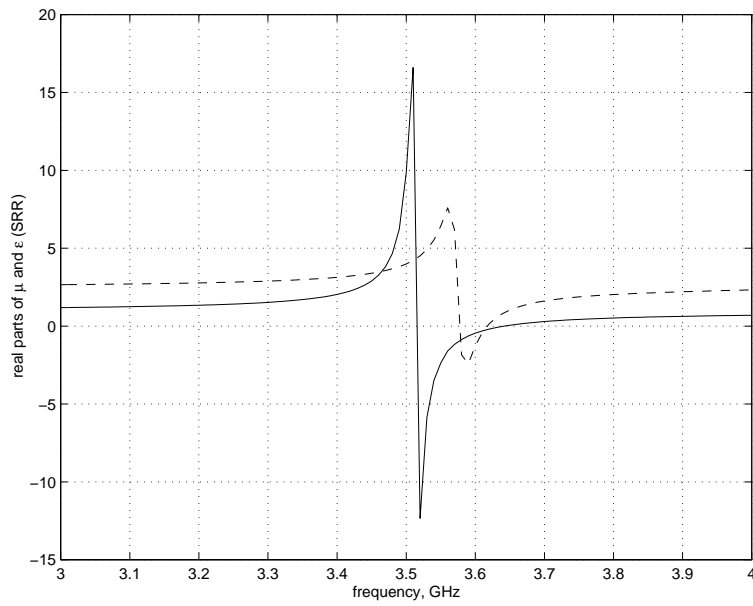


Figure 12: Real parts of the permeability (solid) and permittivity (dashed) of the SRR composite from cubic cells versus frequency. Analytical model.

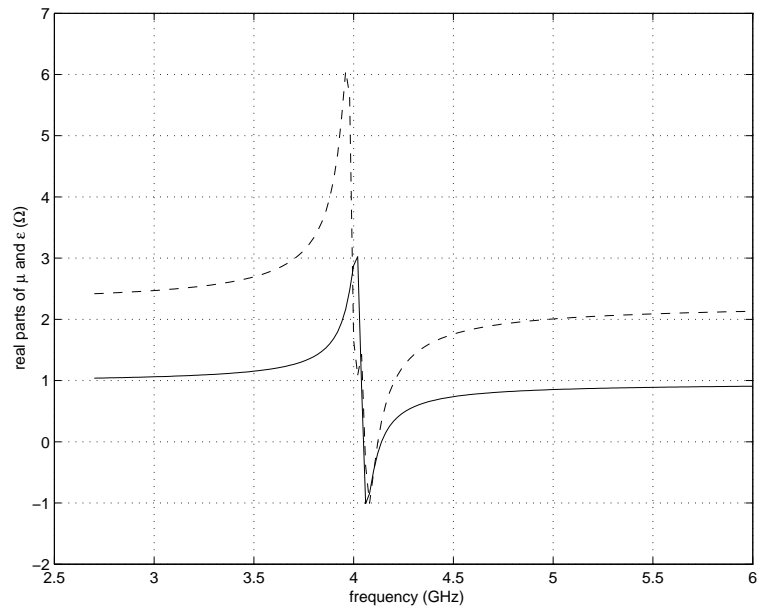


Figure 13: Real parts of the effective permeability (solid) and permittivity (dashed) of an Omega composite formed by cubic cells versus frequency. The host permittivity is 2 and the length of a unit cell is 6.5 mm

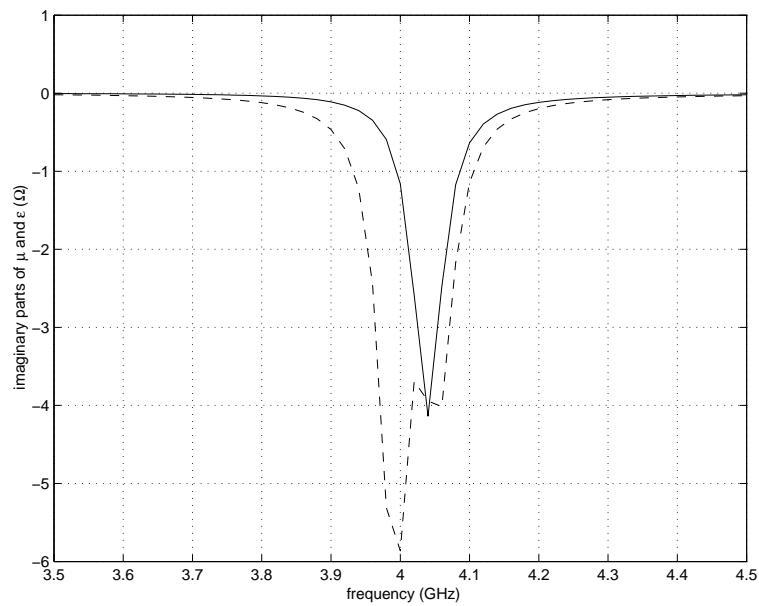


Figure 14: Imaginary parts of the effective permeability (solid) and permittivity (dashed) of an Omega composite formed by cubic cells versus frequency. The host permittivity is 2 and the length of a unit cells is 6.5 mm

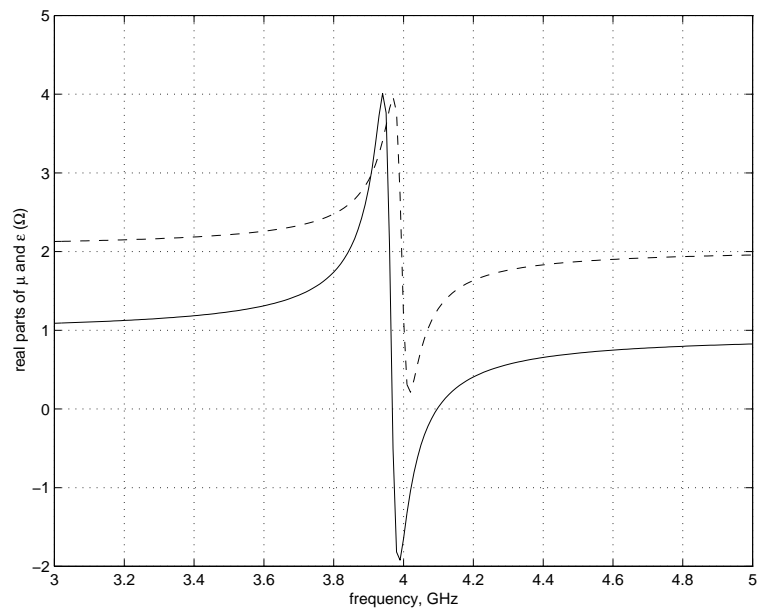


Figure 15: Real part of the effective permeability (solid) and permittivity (dashed) of a random Omega composite. The host permittivity is 2.